Lipid Bilayer Deformation and the Free Energy of Interaction of a Kv Channel Gating-Modifier Toxin

Chze Ling Wee,* David Gavaghan,† and Mark S. P. Sansom*
*Department of Biochemistry and †Computing Laboratory, University of Oxford, Oxford, United Kingdom

ABSTRACT A number of membrane proteins act via binding at the water/lipid bilayer interface. An important example of such proteins is provided by the gating-modifier toxins that act on voltage-gated potassium (Kv) channels. They are thought to partition to the headgroup region of lipid bilayers, and so provide a good system for probing the nature of interactions of a protein with the water/bilayer interface. We used coarse-grained molecular dynamics simulations to compute the one-dimensional potential of mean force (i.e., free energy) profile that governs the interaction between a Kv channel gating-modifier toxin (VSTx1) and model phospholipid bilayers. The reaction coordinate sampled corresponds to the position of the toxin along the bilayer normal. The course-grained representation of the protein and lipids enabled us to explore extended time periods, revealing aspects of toxin/bilayer dynamics and energetics that would be difficult to observe on the timescales currently afforded by atomistic molecular dynamics simulations. In particular, we show for this model system that the bilayer deforms as it interacts with the toxin, and that such deformations perturb the free energy profile. Bilayer deformation therefore adds an additional layer of complexity to be addressed in investigations of membrane/protein systems. In particular, one should allow for local deformations that may arise due to the spatial array of charged and hydrophobic elements of an interfacially located membrane protein.

INTRODUCTION

The interface between a lipid bilayer and bulk water is a complex environment (1) that is exploited by a number of membrane-bound proteins, including monotopic membrane protein enzymes (2,3), signaling proteins (4), and toxins (5). Although x-ray crystallography provides structures of the isolated protein molecules, a detailed model of the interactions of such proteins with the interface must be approached via spectroscopic (6) and/or computational (7) methods. In particular, it is often uncertain how deeply a membrane-associated protein may penetrate into the lipid bilayer. It is therefore of both physicochemical interest and biological importance to more fully characterize the interactions of such proteins with the water/bilayer interface.

A biophysically important example of such proteins is provided by the gating-modifier toxins that act on voltage-gated potassium (Kv) channels, a class of integral membrane proteins that play a central role in the physiology of electrically excitable cells (8,9). They are activated by a change in transmembrane (TM) voltage (from polarized to depolarized), which results in a switch from a functionally closed to an open state (''gating''). Gating-modifier toxins are of particular interest because they can be used to probe the structure and orientation of the voltage sensor (VS), i.e., the domain of Kv channels that moves in response to changes in TM voltage (5,10–28). For example, VSTx1 has been shown to inhibit the archaebacterial channel KvAP by binding to the VSs, thus stabilizing the channel in an open state (11,12,24,26,29). VSTx1 is a small water-soluble protein (34 residues) that is stabilized by three internal disulfide bridges (26). The structure of VSTx1 is such that one-half of its molecular surface is almost exclusively hydrophobic, whereas the other half is hydrophilic and carries a net positive charge of +3 (at the default protonation state for pH 7). This architecture is conserved across related gating-modifier toxins, including HaTx1 and SGTx1 (5,24). Although the exact mechanism of inhibition of KvAP remains uncertain, it is known that the binding site of VSTx1 is confined to the VS domain of KvAP, because the isolated VS is equally effective at binding VSTx1 as the intact KvAP channel (12) and the VS domain and toxin sensitivity may be interchanged between channels (16).

It is thought that VSTx1 interacts with the VS of KvAP by first partitioning into the headgroup/water interface of a lipid bilayer (24,26,28). Given the amphipathic nature of the toxin surface, an interfacial location would not be surprising because this would allow the hydrophobic residues of the toxin to interact with the lipid tails and the more polar residues to interact with the lipid headgroups. It seems that for VSTx1 and its homologs, membrane partitioning serves primarily to provide access to the target VS. Thus, a fuller description of the nature of the mechanism of toxin/bilayer interactions may provide a window into the location of the VS relative to the lipid bilayer.

We recently used atomistic molecular dynamics (MD) simulations to show that VSTx1 (30) and SGTx1 (31) prefer a location close to the headgroup/water interface of the bilayer. However, the free energy and detailed molecular mechanism for the partitioning of a gating-modifier toxin into a bilayer remains to be characterized. Recent developments in coarse-grained (CG) simulation methodology (32–45) make it feasible to probe membrane protein systems over

Submitted February 4, 2008, and accepted for publication July 3, 2008.

Address reprint requests to Mark S. P. Sansom, Dept. of Biochemistry, University of Oxford, South Parks Road, Oxford OX1 3QU, UK. Tel.: 44-1865-275371; Fax: 44-1865-275373; E-mail: mark.sansom@bioch.ox.ac.uk.

Editor: Kenton J. Swartz.

0006-3495/08/10/3816/11 $2.00
doi: 10.1529/biophysj.108.130971

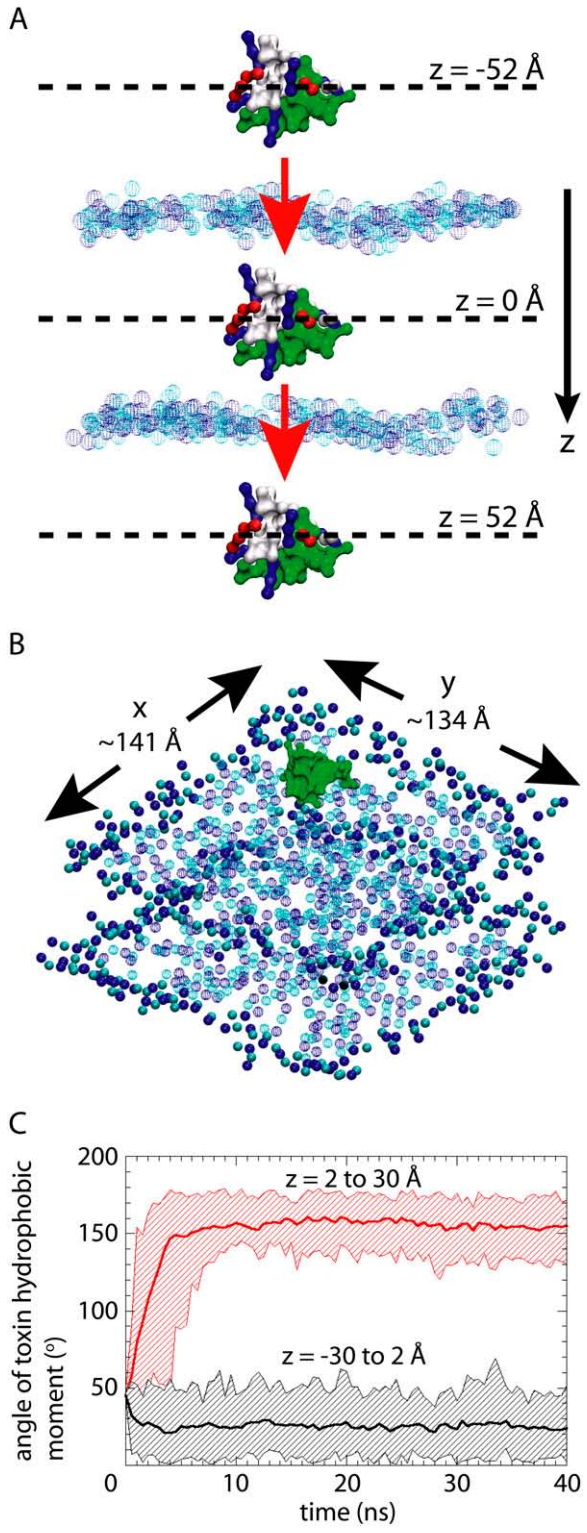

FIGURE 1 Experimental setup and validation of approach. (*A*) Umbrella sampling. The reaction coordinate is along the bilayer normal; 104 independent windows spaced 1 Å apart were used to sample from bulk, across the bilayer, and into bulk again ($z = -52$ to 52 Å). The bilayer center is at $z \sim 0$ Å. An identical initial orientation of the toxin with respect to the bilayer (as shown) was used in all windows. (*B*) Setup details specific to VSTX-PC-free. The lipids at the edge of the bilayer, which represents a border of thickness 15 Å, had a positional restraint applied on their phosphates in *x*, *y*, and *z*. All other lipids had no restraint applied. (*A*) The hydrophobic, basic, acidic, and polar residues of the toxin are colored green, blue, red, and white, respectively. (*B*) All toxin residues are colored green for clarity. The phosphate and choline groups of the lipids (POPC bilayer shown) are colored dark blue and light blue, respectively, in a dotted scheme. In *B* the phosphate and choline groups of the restrained lipids at the edge of the bilayer are identically colored but in a solid scheme. Other lipid particles, waters, and counterions are omitted for clarity. (*C*) Angle of hydrophobic moment of the toxin (i.e., a measure of toxin orientation) with respect to the bilayer normal in VSTX-PC-free (first 40 ns per window shown). The thick lines represent the average over windows $z = -30$ to 2 Å (black) and $z = 2$ to 30 Å (red). The region between the upper and lower limits of each set is shaded in.

extended timescales. Microsecond timescales have been reported for a range of systems (44,46–48). Here, we utilize umbrella sampling with a CG protein and lipid model, for a total simulation time in excess of 30 μs, to compute the one-dimensional (1D) potential of mean force (PMF) that describes the interaction between VSTx1 and 1), a zwitterionic palmitoyl-oleoyl-phosphatidyl choline (POPC) bilayer; and 2), an anionic bilayer (a 3:1 mixture of palmitoyl-oleoyl-phosphatidyl ethanolamine (POPE) and palmitoyl-oleoyl-phosphatidyl glycerol (POPG)). We reveal the free energy preference for the toxin to partition into the headgroup/water interface. Furthermore, we observe significant deformations in the bilayer due to the toxin, which perturbs the free energy profile. This is of interest in the context of the theoretical literature on proteins and bilayer distortions (49,50). In particular, such deformations of the bilayer inform our thinking concerning the likely plasticity of the membrane as a whole during interactions of proteins at the water/bilayer interface.

THEORY AND METHODS

Simulation systems

We are aware of the dynamic nature of a membrane system, and thus were concerned with possible problems regarding sampling and convergence that may arise from this. We therefore considered two simulation protocols in our estimations of PMFs. The first protocol used a constrained system in which we limited any possible deformation of the bilayer due to the positively charged toxin. This was applied to the interaction of the toxin with both POPC and 3:1 POPE/POPG bilayers (VSTX-PC and VSTX-PEPG). In both VSTX-PC and VSTX-PEPG, a positional restraint was applied on the *z*-coordinate of all lipid phosphates (note that the bilayer normal is along the *z* axis of the simulation box). We then repeated the calculations with the POPC bilayer with the limitations on bilayer deformation removed (VSTX-PC-free), such that in VSTX-PC-free only those phosphates at the outer edge of the bilayer (representing a border of thickness 15 Å) were position restrained (in *x*, *y*, and *z*, Fig. 1 *B*). The lipids at the border can be thought to be sufficiently far away from VSTx1 that their interaction with the toxin is negligible. All other lipids in VSTX-PC-free had no restraint applied (i.e., the lipids close to VSTx1 were free to deform as they interacted with the toxin). The center of mass (c.o.m.) of VSTx1 was additionally restrained in *x* and *y* in VSTX-PC-free.

Calculation of PMF

Our reaction coordinate for calculation of the PMF is the position of the toxin along the bilayer normal, which corresponds to the *z* axis of our simulation box (Fig. 1 *A*). The PMF along *z* is the constrained free energy and is defined (51) as:

$$W(z) - W(z') = -\int_{z'}^{z} d\zeta \langle F(\zeta) \rangle = -kT \ln \frac{\int d^{3N-1}\mathbf{R}\, e^{-U(\mathbf{R},z)/kT}}{\int d^{3N-1}\mathbf{R}\, e^{-U(\mathbf{R},z')/kT}},$$

where k is the Boltzmann's constant, T is the temperature, and U is the potential energy as a function of z and the $3N$-1 remaining coordinates, $\mathbf{R}$.

To perform umbrella sampling, we used 104 independent windows along z spaced 1 Å apart for each system to sample from bulk, across the bilayer, and into bulk again ($z = -52$ to 52 Å, the bilayer center is at $z \sim 0$ Å, Fig. 1 *A*). For each window, a simulation of duration 40 ns was employed in VSTX-PC and VSTX-PEPG, and a duration of 240 ns was used in VSTX-PC-free. An identical initial orientation of the toxin with respect to the bilayer was used in all windows for all systems (as shown in Fig. 1 *A*). Initial bilayer models were generated by self-assembly (46), starting with a box of randomly positioned lipids and water, and followed by a production MD run of 200 ns (Supplementary Material, Data S1). Our self-assembled bilayer consisted of 256 lipids with surface dimensions of ~95 × 89 Å and 91 × 86 Å in VSTX-PC and VSTX-PEPG, respectively. A larger bilayer with surface dimensions of ~141 × 134 Å and 581 lipids was self-assembled in VSTX-PC-free (Fig. 1 *B*).

To position VSTx1 in the bilayer, we used a protocol similar to that employed in previous studies of related toxins (30,31). Briefly, we ''grew'' the toxin in the bilayer by gradually scaling the coordinates of VSTx1 to its full size in five steps, with 100 steps of steepest-descent energy minimization at each step to allow the lipids to adjust their conformations to host the toxin. The lipid coordinates from each previous step were kept while the original toxin coordinates were rescaled. At each step, any lipids whose phosphates were within 3.6 Å of any toxin particle were removed. Across all windows for all systems, no more than one lipid per window was removed.

To perform umbrella sampling, the z-coordinate of the c.o.m. of VSTx1 was restrained relative to the z-coordinate of the c.o.m. of the entire bilayer in VSTX-PC and VSTX-PEPG with a harmonic umbrella potential. In VSTX-PC-free, this was relative to the lipids at the edge of the bilayer. All toxin and lipid restraints, and the umbrella potential, utilized a force constant of 10 kJ mol^{-1} Å^{-2}.

Given the restraints on the lipid phosphates, and on the toxin in VSTX-PC-free, we are therefore not integrating over all $3N$-1 remaining coordinates. Thus, the free energy profiles of VSTX-PC and VSTX-PEPG are such that the lipids cannot displace significantly along z. Similarly, the profile of VSTX-PC-free is such that the lipids at edge of the bilayer cannot displace significantly in x, y, or z, and the toxin cannot drift significantly along the plane of the bilayer surface. We do not expect the VSTX-PC-free profile to differ significantly from one derived from a setup in which a full integral over all $3N$-1 remaining coordinates is performed.

The biased probability distributions were combined and unbiased using an implementation of the weighted histogram analysis method (WHAM) (52) (http://membrane.urmc.rochester.edu/). The free energy profiles presented in this article were generated with the final 5 ns of simulation data per window.

CG simulations

We used a CG protein model (44,46,47) in which an average 4-to-1 mapping of heavy atoms is used, i.e., each amino acid is represented by one CG backbone particle and between 0 and 2 CG side-chain particles depending on residue size. The CG model has been shown to be able to reproduce data derived from experiments and atomistic simulations for a number of membrane proteins and synthetic α-helical peptides (47). Transfer free energies of individual neutral amino acid side-chains from water to cyclohexane have also been shown to correlate well with experimental data (53). The CG lipid model has also been shown to be able to reproduce structural properties of membranes derived from experiments (54). VSTx1 was treated as a semirigid body, with harmonic restraints (force constant 10 kJ mol^{-1} Å^{-2}) applied between all toxin particles which were within 7 Å of each other. This assumption is supported by recent atomistic simulations of VSTx1 in an aqueous environment where the toxin remained structurally stable, with a C_α root mean-square deviation (RMSD) that did not exceed 3 Å over a 10 ns timescale (30).

MD simulations were performed using GROMACS 3.2.1 (55,56) (www.gromacs.org). VSTx1 was kept in the default protonation state for pH 7. Cl^- or Na^+ counterions were added to keep each system electrically neutral. VSTx1, bilayer, water, and counterions were temperature-coupled with a Berendsen thermostat (57) with a weak coupling constant of 1.0 ps and a reference temperature of 310 K. Electrostatic (Coulombic) interactions was smoothly shifted to zero between 0 and 12 Å and utilized a relative dielectric constant of 20, and van der Waal's interactions were smoothly shifted to zero between 9 and 12 Å. Semiisotropic pressure coupling with a Berendsen barostat (57) in x and y at 1 bar with a coupling constant of 1.0 ps and a compressibility value of 5.0×10^{-6} bar^{-1} was used. Our simulations utilized a TM potential of 0 V (i.e., no TM voltage was applied). The time step of integration was 0.04 ps.

RESULTS

Toxin and bilayer in the free energy simulations

It is important to ascertain whether the $3N$-1 degrees of freedom that are not explicitly sampled equilibrate before collecting distributions along z. Since it is impractical to investigate all $3N$-1 degrees of freedom, we approximate this by probing only the important degrees of freedom. The amphipathic molecular surface of VSTx1 means the orientation of the toxin with respect to the bilayer is likely to influence our estimations of PMFs. Thus, we probed the orientation of the toxin in the bilayer. Fig. 1 *C* shows the variation in the hydrophobic moment (58) of the toxin (i.e., a measure of toxin orientation) with respect to the bilayer normal for windows $z = -30$ to 30 Å in VSTX-PC-free for the first 40 ns per window. We display the time evolution of the hydrophobic moment averaged over windows $z = -30$ to 2 Å and $z = 2$ to 30 Å separately. The bilayer center is at $z \sim 0$ Å. The angle of the hydrophobic moment of the toxin equilibrates to two distinct values by ~10 ns, an average of 24.8 ± 11.4° for windows $z = -30$ to 2 Å and an average of 155.8 ± 11.2° for windows $z = 2$ to 30 Å (averages ± SD taken over 10 to 240 ns per window). Thus, the toxin is able to reorient as it crosses the approximate bilayer center. The two equilibrated values correspond to the hydrophobic face of VSTx1 being exposed to the hydrocarbon tail region of the bilayer, with its hydrophilic face positioned to interact with the lipid headgroups (24,26,30). In particular, the three Trp residues on the hydrophobic patch of the toxin (W7, W25, and W27) are exposed to the hydrophobic phase of the bilayer, consistent with previous studies (26). In addition, L30 of the toxin, centered on the hydrophobic patch, is also directed toward the lipid tails, which is consistent with depth-dependent fluorescence quenching data (for W30) on HaTx1 (59). For windows sufficiently far away from the bilayer that the interaction between the bilayer and the toxin is minimal ($z = -52$ to ~ −40 Å and $z \sim 40$ to 52 Å), the hydrophobic moment of the toxin fluctuated over a wide range without equilibrating. However, the smoother energy landscape associated with a CG potential, which is likely to speed up the dynamics of a system (38), coupled with relatively long simulation times,

meant that we were able to probe a large number of possible orientations of the toxin to ensure well-converged PMF profiles.

In VSTX-PC-free, the bilayer deforms as it interacts with the toxin. Such deformations could influence the free energy profile and therefore must equilibrate before sampling. We monitored the displacement (along the bilayer normal) of the lipid phosphates near the toxin, separately for the upper and lower leaflets of the bilayer (Supplementary Material, Data S1). We show that the displacements of the lipid phosphates of both leaflets equilibrated by 80 ns in all windows (bilayer deformation is discussed in detail later). Thus, the bilayer deforms due to the toxin but achieves dynamic equilibrium. Overall, we obtain evidence of sufficient equilibration of two important degrees of freedom, which provides confidence that 1D umbrella sampling can be performed on a system as complex as ours.

We adopted a systematic approach to evaluate convergence of our free energy profiles. We split the final 5 ns per window (i.e., 35–40 ns per window in VSTX-PC and VSTX-PEPG, and 235–240 ns per window in VSTX-PC-free) into 10 × 0.5 ns blocks and systematically incremented the number of blocks used to generate the PMF profiles. We showed that the variation between profiles was statistically insignificant (Supplementary Material, Data S1).

Free energy profiles

Fig. 2 shows the free energy profiles for positioning VSTx1 at different positions along the bilayer normal. We first focus on VSTX-PC and VSTX-PEPG, where energy wells are present at a distance of 21 and 24 Å, respectively, from the bilayer center, corresponding to a location at the headgroup/water interface. The magnitude of the well with respect to bulk (averaged across both halves for each profile) is 26.5 and 34 kcal/mol in VSTX-PC and VSTX-PEPG, respectively. It is therefore more favorable for VSTx1 to partition into the interfacial region of both bilayers than to remain in an aqueous environment. Given the amphipathic nature of VSTx1, this may not be surprising because there is an energetic preference for the hydrophobic surface residues of the toxin to minimize their exposure to waters. The hydrophilic residues of the toxin have been shown to form hydrogen bonds with the lipid phosphates, and with the ethanolamine and head glycerol moieties of POPE and POPG lipids, respectively (30). Thus, the interfaces of both bilayers are able to mimic the hydrogen-bonding environment provided by the waters. The free energy of desolvation of the hydrophobic residues of VSTx1 is therefore likely to be a major contributor to the interfacial wells. Although hydrogen-bonding interactions are not explicitly represented in the CG model, they are indirectly captured by the parameterization of the CG force field (35).

The biophysical implication is that VSTx1 is likely to accumulate in high concentrations in the membrane. Post partitioning, it is unlikely for the toxin to departition into the aqueous environment. Furthermore, there is a significant free energy barrier (from average well to profile peak) for the toxin to cross the approximate bilayer center: 61 and 77 kcal/mol in VSTX-PC and VSTX-PEPG, respectively. The interfacial wells and central barrier suggest that the toxin is likely to be confined to a location close to the interfacial region of the bilayer toward the extracellular solvent. Thus, it is unlikely that VSTx1 would be able to cross the membrane center, at least when the toxin interacts with the membrane. This would suggest that the S3b-S4a region of the VS of KvAP is similarly located close to the interface, at least when the channel is in a state (open) that binds VSTx1. The 7.5 kcal/mol difference in the magnitude of the wells and the 16 kcal/mol difference in the magnitude of the barrier between VSTX-PC and VSTX-PEPG can be reconciled if one considers that the positively charged toxin is able to form stronger interactions with the overall anionic 3:1 POPE/POPG bilayer.

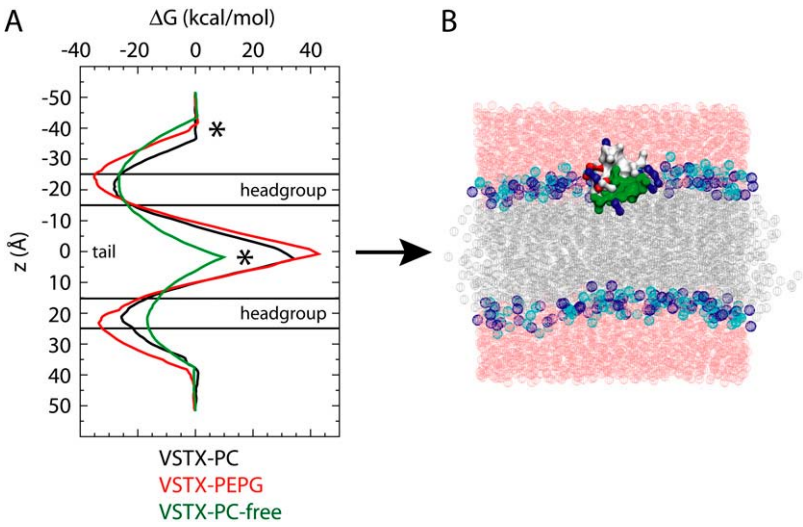

FIGURE 2 PMF profiles. The approximate location of the headgroup and tail region of the bilayer is shown; Asterisks highlight the main differences between VSTX-PC and VSTX-PC-free. The image shows the toxin in a POPC bilayer at the free energy well. The color scheme for the toxin is identical to Fig. 1 *A*. The phosphate and choline groups of the lipids are colored dark blue and light blue, respectively, in a dotted scheme. All other lipid particles are colored gray. Waters are shown in pink. Counterions are not shown.

We therefore show that the strength of interaction between VSTx1 and a bilayer is dependent on lipid species. This may provide insights into the reported experimental discrepancies on the degree of interaction between VSTx1 and zwitterionic and anionic bilayers (24,26). Given that the amphipathic molecular architecture of VSTx1 is conserved across other gating-modifier toxins (5), this suggests that membrane partitioning may be a common feature of these toxins and a component of the mechanisms of channel inhibition.

We now compare VSTX-PC with VSTX-PC-free, where limitations on bilayer deformation have been removed, to reveal two main differences (Fig. 2): 1), broadening of the free energy wells; and 2), a significant reduction, by 28.5 kcal/mol, in the central barrier. When the toxin was distant from the bilayer surface (e.g., $z = -45$ to -44 Å; Fig. 3 *A*), the bilayer was unperturbed, with fluctuations in the displacement of the lipid phosphates of the upper leaflet of <3 Å. As the toxin approached the bilayer surface more closely ($z = -44$ to -43 Å; Fig. 3 *B*), the bilayer ''buckled'' outward to capture the toxin and thus resulted in an earlier stabilization of the toxin along z. Specifically, the bilayer deformed so as to optimize the interaction of its headgroups with the hydrophilic residues of the toxin, while burying the hydrophobic patch of the toxin within the lipid tails. The lipid phosphates of the upper leaflet thus displaced by up to a maximum of ~18 Å to capture the toxin. The angle of the hydrophobic moment of the toxin (relative to z) was quickly stabilized to an average of 16.8 ± 7.4° (averaged over 10–240 ns). As the toxin was dragged into the tail region of the bilayer, the upper leaflet deformed inward to minimize the energetic penalty of placing the charged toxin in what would otherwise be a predominantly hydrophobic environment of an unperturbed bilayer (Fig. 3 *C*). Upon crossing the approximate bilayer center, the grip on the toxin was transferred from the upper to the lower leaflet (Fig. 3 *D*). The angle of the hydrophobic moment of VSTx1 mirrored this transition, switching from an average of 22.4 ± 11.5° to 162.9 ± 8.8°. The lipid phosphates of both leaflets displaced by up to a maximum of 14 Å to minimize the exposure of the charged residues of the toxin to the hydrophobic core of the bilayer. Note that in all three cases (Fig. 3, *B–D*) the displacements decayed to background (i.e., as in the unperturbed bilayer; Fig. 3 *A*) well before the restrained edges of the box, suggesting that periodicity artifacts are unlikely to unduly influence these conclusions.

The free energy wells in VSTX-PC-free were located at 21–23 Å from the bilayer center, consistent with VSTX-PC. Despite the reduction in the central barrier in VSTX-PC-free, a central barrier of 32.5 kcal/mol still exists (relative to the average well), and this will prevent VSTx1 from translocating across the width of the membrane. Relative to bulk solvent, it is still more unfavorable for the toxin to be buried close to the center of the bilayer by 11.5 kcal/mol in VSTX-PC-free. It is interesting to note that the free energy profile in VSTX-PC-free is not symmetrical about the bilayer center. In

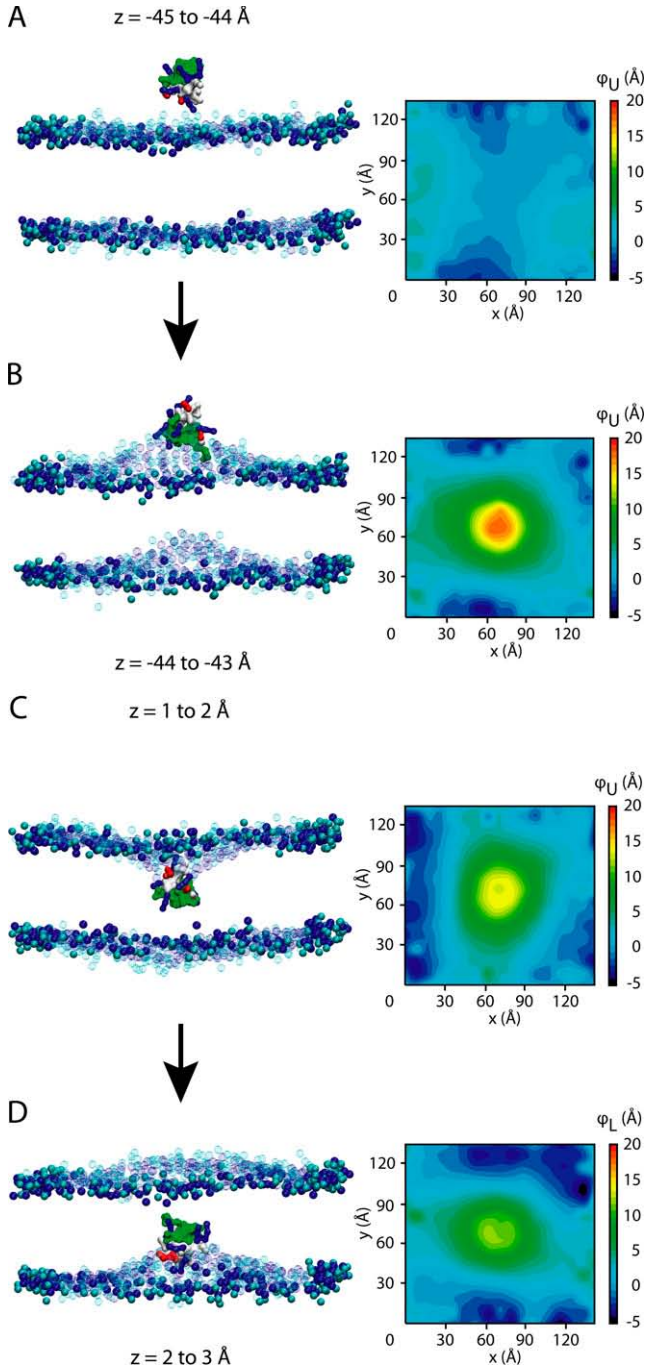

FIGURE 3 Bilayer deformation (VSTX-PC-free). (*A* and *B*) Dynamics as the toxin approaches the bilayer surface. (*C* and *D*) Dynamics as the toxin crosses the bilayer center. Snapshots were taken at (*A* and *B*) 40 ns and (*C* and *D*) 30 ns. The contour plots show the average displacement along the bilayer normal of the lipid phosphates of either the upper (ϕ_U) or lower (ϕ_L) leaflet for the respective window (averaged over 80–240 ns, relative to the phosphates of the restrained lipids at the edge of the bilayer). For convenience of representation, the displacement values of the contour plot of window $z = 1$ to 2 Å (*C*) are multiplied by -1. The color scheme for the toxin is identical to Fig. 1 *A*. The color scheme for the bilayer is identical to Fig. 1 *B*. Waters and counterions are not shown.

particular, the magnitudes of the free energy wells in VSTX-PC-free differ significantly (26 vs. 17 kcal/mol), resulting in an average well of 21.5 kcal/mol. We noted that the self-assembly procedure (Supplementary Material, Data S1) yielded different numbers of lipids in the upper and lower leaflets of the bilayer in VSTX-PC-free (287 and 294 lipids) respectively, which enabled us to explore the influence of lipid packing density on VSTx1/bilayer interactions. Thus, the lack of symmetry in the VSTX-PC-free free energy profile suggests that the lipid packing density may have some effect on the degree of bilayer deformation (as discussed later), and consequently the free energy profile. This indicates that free energy profiles may be sensitive to only a ~2% difference in the number of lipids between the leaflets. This is in agreement with earlier theoretical studies that indicated that the surface tension exerted on integral membrane proteins would be sensitive to the overall shape of the lipid molecules present in the bilayer (60).

Bilayer deformation

To further probe the behavior of the bilayer due to the toxin, we plot in Fig. 4 *A* the average distance between the lipid phosphates of the upper and lower leaflets (d_{pp}) as a function of toxin position along the bilayer normal in VSTX-PC-free. We defined a cylindrical region of bilayer of radius 20 Å, centered on the initial *xy*-coordinates of the c.o.m. of the toxin (the long axis of the cylinder is along the bilayer normal). The distances were averaged spatially over this region and over the final 160 ns per window. In windows where the toxin is sufficiently far away that its interaction with the bilayer is minimal, d_{pp} was 42 Å, which is within the range observed for a POPC bilayer in atomistic simulations (61). As the toxin approached the bilayer surface, the bilayer stretched along its normal by 4–5 Å. At the preferred toxin depth of 21–23 Å from the bilayer center, there was no noticeable deformation of the bilayer. Conversely, the bilayer thinned by up to ~3 Å to accommodate the placement of the charged toxin within its hydrophobic core. In Fig. 4 *B*, we plot the average displacement of the lipid phosphates (δ) of the upper (δ_U) and lower (δ_L) leaflets again as a function of toxin position along the bilayer normal. The displacements were averaged spatially and temporally as per d_{pp}. The observed thickening and thinning of the bilayer can be accounted for by the inequality in the magnitudes of δ_U and δ_L at a certain z value. For example, δ_U was ~14 Å when the c.o.m. of the toxin was at $z \sim -44$ Å. This was not matched by a δ_L value of ~9 Å. We also noted the lack of symmetry about the bilayer center in both plots in Fig. 4, which is mirrored by a similar lack of symmetry in the free energy profile in VSTX-PC-free (Fig. 2). Thus, the degree by which the bilayer deforms influences the free energy profile. The structural flexibility of a POPC bilayer is further emphasized, with lipid phosphate displacements of individual leaflets that approached ~15 Å.

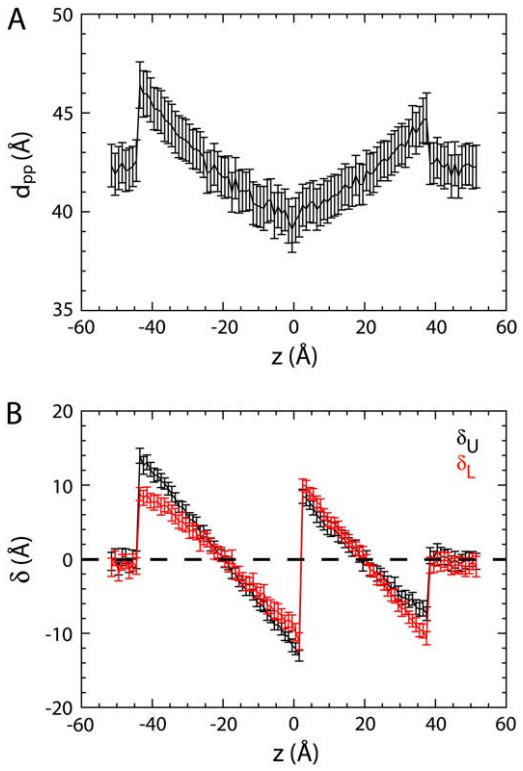

FIGURE 4 Bilayer deformation (VSTX-PC-free). (*A*) Average distance between lipid phosphates of the upper and lower leaflets (d_{pp}) as a function of toxin position along the bilayer normal. (*B*) Average displacement (δ) of lipid phosphates of the upper (δ_U) and lower (δ_L) leaflets as a function of toxin position along the bilayer normal. A cylindrical region of bilayer of radius 20 Å, centered on the initial *xy*-coordinates of the c.o.m. of VSTx1 is defined (the long axis of the cylinder is along the bilayer normal). δ is with respect to the restrained lipids at the edge of the bilayer (Fig. 1 *B*). Averages are taken spatially across this region and over the final 160 ns per window. Bars represent ± SD.

Further examination of the structure of the bilayer in the most deformed cases (i.e., when the toxin is positioned close to the center the bilayer) reveals that in addition to distortion of the bilayer, there was significant local penetration of water molecules into the bilayer in the vicinity of the toxin (Fig. 5). A similar effect has been seen in, e.g., atomistic MD simulations of the PMF of an arginine side chain across a lipid bilayer (62). Indeed, atomistic simulations of the VSTx1 positioned in the center of a bilayer also showed significant local water penetration (C. L. Wee, D. Gavaghan, and M. S. P. Sansom, in preparation). Thus, at a semiquantitative level the CG simulation appears to reproduce this aspect of more detailed atomistic simulations.

Mapping the residues of VSTx1 relative to the membrane

To probe the detailed positions of the residues of VSTx1 relative to the bilayer normal, we clustered the toxin structures over 30–40 ns of window $z = -21$ to -20 Å of VSTX-PC (i.e., when the toxin has located its equilibrium orientation

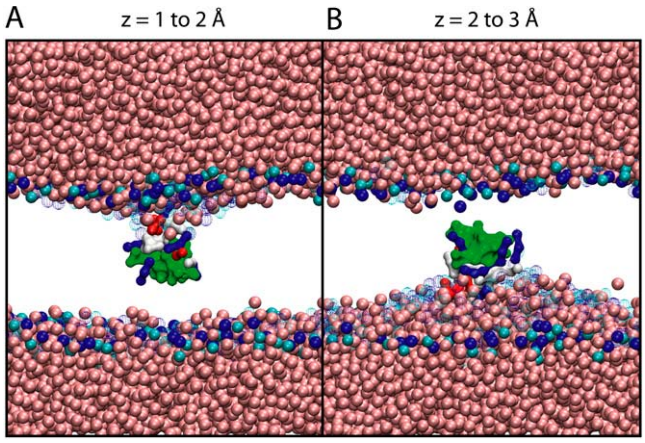

FIGURE 5 Solvation structure of VSTx1 when positioned in the hydrophobic core of the bilayer. The color schemes for the toxin and the bilayer are identical to Fig. 3. CG water particles are shown in pink. Counterions are not shown.

in the membrane and is located at the free energy well). Information on the orientation of the toxin relative to the bilayer was preserved during clustering and the median of the cluster was determined. The median of the cluster represents the most frequently observed equilibrated orientation of the toxin relative to the bilayer normal. The NMR structure of VSTx1 was mapped onto the CG median structure via a least-squared fit of the C_α atoms onto the CG backbone particles. Thus, Fig. 6 *A* depicts the detailed positions of the toxin residues relative to the bilayer when the toxin is located at the free energy well. The hydrophobic patch of VSTx1 can be seen to be exposed to the hydrophobic phase of the membrane. We estimate the c.o.m. of F5, M6, W7, W25, W27, L30, P33, and F34 to be positioned 16.3, 16.2, 19.4, 19.1, 19.6, 16.6, 14.6, and 11.5 Å, respectively, from the bilayer center. The charged residues E1 (24.6), K4 (16.3), K8 (23.6), K17 (21.2), D18 (19.2), R24 (21.9), and K26 (21.3) were positioned to interact favorably with the polar lipid headgroups (distances in Å). K10 (31.9) and D14 (27.3) and the polar residues were exposed to the extracellular solvent. Our predicted orientation of VSTx1 thus allows the charged residues to interact with the lipid headgroups and waters, and the hydrophobic residues to interact with the lipid tails, and is overall consistent with the amphipathic molecular surface of the toxin.

In Fig. 6 *B*, we show the distributions of VSTx1 when located at the free energy well (time-averaged over 10–40 ns of window $z = -21$ to -20 Å of VSTX-PC i.e., the c.o.m. of the toxin is located ~21 Å from the bilayer center), and the VS of KvAP along the bilayer normal. We modeled the orientation of the VS of KvAP in a POPC bilayer via a CG bilayer self-assembly simulation of duration 200 ns, where one molecule of the VS was placed in a simulation box with 550 randomly positioned POPC lipids (42,63) (Supplementary Material, Data S1). A bilayer formed with the VS molecule adopting a TM orientation similar to that previously reported (42) by 20 ns (the VS distributions were time-averaged over 50–200 ns). The distributions of the residues of VSTx1 that are thought to be important for binding the VS of KvAP (26), and the distributions of the residues of the VS that have been shown via a mutagenesis study to be important for binding VSTx1 (16) are shown. It can be seen that there is a degree of overlap along the bilayer normal of the hydrophobic residues of the toxin and a stretch of leucines on S3b/S4a ''paddle'' motif of the VS. In particular, F5, W7, and W27 of VSTx1 are positioned in close proximity to these leucines. K4 and S22 on the toxin are positioned to interact with the polar H109 on the VS. Overall, our results support the notion that VSTx1 partitions to the membrane/water interface at the extracellular side, where it interacts with the ''paddle'' motif of the VS, which is similarly located close to the extracellular interface, as supported by recent crystal structures of Kv channels (15).

DISCUSSION AND CONCLUSIONS

PMF calculations have been previously used to probe a number of ion channel-related phenomena, including ion permeation through the selectivity filter of a K^+ channel (64), hydrophobic gating in the nicotinic-acetylcholine receptor (65), and free energy profiles of amino acid side-chains as a function of depth in a bilayer (62,66). Here, we performed PMF calculations with a CG protein and lipid model to study the interaction between VSTx1 and two different phospholipid bilayers. The toxin/bilayer system is sufficiently simple and tractable to allow one to study the nature of the interaction of the bilayer with a charged peptide/protein. Preliminary atomistic simulations of a similar system, with VSTx1 in a nonoptimal starting orientation in a bilayer, suggest that this system reaches equilibrium very slowly. This is revealed by, e.g., a slow drift in the orientation of the toxin over multiple 20 ns atomistic simulations. Given that it is important for nonsampled degrees of freedom to equilibrate quickly when a PMF calculation is being performed, this necessitates the use of a CG protein and lipid model.

Our free energy profiles reveal the preference for the toxin to partition into the headgroup/water interface of a bilayer, in qualitative agreement with recent experimental studies (28). Using the theoretical framework of Ben-Tal et al. (67), we used our PMF profiles to estimate binding constants of $\sim 10^{19}$, $\sim 10^{23}$, and $\sim 10^{18}$ for VSTX-PC, VSTX-PEPG, and VSTX-PC-free, respectively, which is orders of magnitude larger than that reported experimentally for VSTx1 (24,28) and related toxins (68). This difference is somewhat puzzling. We therefore tested whether it arises from the CG approximation or reflects a more general discrepancy between experimental and theoretical estimates of partitioning energetics.

To test the former possibility (i.e., the CG approximation), we performed the following simple test calculation: Assuming that VSTx1 is located in its free energy well at the

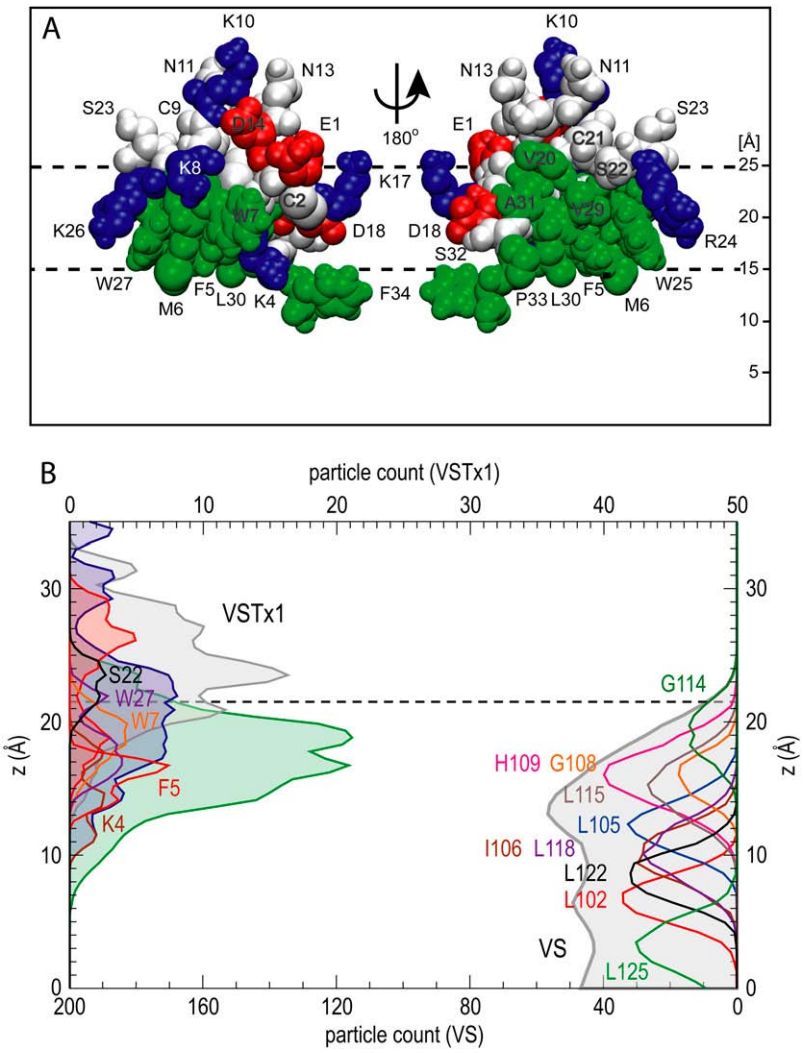

FIGURE 6 (*A*) Equilibrium positions of the residues of VSTx1 (relative to the bilayer) with the toxin located at the free energy well. Distances are measured relative to the center of the bilayer ($z \sim 0$ Å). The c.o.m. of VSTx1 is located ~21 Å away from the bilayer center. The horizontal dotted lines indicate the approximate headgroup region of the bilayer. The color scheme for the toxin is identical to Fig. 1 *A*. (*B*) Distributions of side chains of VSTx1 and the VS domain of KvAP along the bilayer normal. The toxin distributions were averaged over 10–40 ns of window $z = -21$ to -20 Å of VSTX-PC and have been scaled by a factor of 10 to improve clarity. The hydrophobic, basic, acidic, and polar residues of the toxin are shown in green, blue, red, and white, respectively, and are colored in. K4, F5, W7, S22, and W27 of VSTx1, thought to be important for binding the VS of KvAP (26), are shown separately. The VS distributions were averaged over 50–200 ns of a CG bilayer self-assembly simulation in which one molecule of the VS of KvAP was placed in a simulation box with randomly positioned POPC lipids (see main text for details). A bilayer formed with the VS molecule adopting a TM orientation by 20 ns. The VS (scaled by a factor of 10) is shown in white. Residues important for binding VSTx1 (16) (scaled by a factor of 100) are shown separately. The location of the peaks of the lipid headgroup distributions is shown as a horizontal dotted line. Distances are measured relative to the center of the bilayer ($z \sim 0$ Å).

membrane/water interface, we used the average position of each residue of the toxin along the bilayer normal in combination with recent atomistic single amino-acid PMFs across a bilayer (69,70) and the assumption of a simple additive sum to obtain a free energy well depth of ~23 kcal/mol. This is of comparable magnitude to our CG estimate (e.g., ~27 kcal/mol in VSTX-PC). Furthermore, our own preliminary data (C. L. Wee, D. Gavaghan, and M. S. P. Sansom, in preparation) from atomistic PMF simulations in which we recalculated the 1D free energy profile (along the bilayer normal) of VSTx1 interacting with a POPC bilayer give an interfacial free energy well of ~23 kcal/mol. Thus, the difficulty does not seem to reside in the CG approximation to the energetics. This suggests a discrepancy between experimentally estimated binding constants and simulation-derived values (regardless of whether one employs CG or atomistic simulations). Further studies, both by us and by others, will be required to understand this difference.

Overall, the simulated membrane partitioning reflects the molecular architecture of VSTx1 and is likely instrumental in its role as a gating-modifier toxin. Given that only several residue pairs between the VS and toxin are thought to interact (5), and that an apparent high-affinity inhibition has been reported (12,24), our result supports recent suggestions that a significant component of the binding energy between VSTx1 and KvAP may be accounted for by the nonspecific free energy of membrane partitioning because the direct toxin-channel interaction does not need to be strong (12,24). A membrane-access mechanism may also explain the apparent slower binding kinetics for VS toxin-channel versus pore blocker toxin-channel interactions (5).

We show that the bilayer can deform significantly around the positively charged toxin, and that such deformations perturb the free energy profile. Deformation has also been reported in, e.g., atomistic simulations of a bilayer containing a charged S4 helix (71), and in both atomistic and CG simulations of the VS domain of KvAP inserted into lipid bilayers (42,72). Here, we report more considerable deformation of a bilayer due to a gating-modifier toxin when the system is in a state of non-equilibrium. It is interesting that recent NMR

and neutron diffraction results indicate that VSTx1 may cause alterations in membrane structure and dynamics (73). Thus, a view emerges in which the bilayer is a malleable body that may reconfigure its local structure to allow otherwise energetically unfavorable events to occur. Of interest, our results suggest a degree of sensitivity of bilayer deformation to lipid packing density. The packing of the lipids in a bilayer is dependent on lipid species, and additionally on the presence of other molecules, e.g., cholesterol. It may therefore be of interest to model more complex mixed-lipid environments in future studies of toxins and other membrane proteins.

We must consider possible limitations of our approach. Although CG models are approximate (74), they have been used successfully to characterize the interactions of peptides (47) and proteins (63) with lipid bilayers to probe lipid bilayer deformation by integral membrane proteins (42,44), and to explore bilayer/protein coupling in gating of mechanosensitive channels (48). It is therefore important to explore the strengths and weakness of such approaches. Perhaps the most marked simplification is that of water. In the CG model used in this study, four water molecules are represented as one CG particle (35). Snorkeling of water molecules into the tail region of a bilayer has been reported in atomistic simulations where, e.g., a protonated arginine residue is buried in the hydrophobic core (62). Such effects could provide a micropolar environment for the charged residues of VSTx1 and, as shown in Fig. 5, can (albeit to a limited extent) be observed in our CG simulations. However, additional waters that are able to penetrate the hydrophobic core, as observed in atomistic simulations, are likely to additionally stabilize the toxin in the bilayer (C. L. Wee, D. Gavaghan, and M. S. P. Sansom, in preparation) and could therefore modify the free energy profile. However, preliminary PMF profiles derived from our atomistic simulations show similar global features to the profiles presented in this study (C. L. Wee, D. Gavaghan, and M. S. P. Sansom, in preparation). Specifically, the overall shape of the profile is preserved in the atomistic PMF although the magnitude of the central barrier is reduced. Thus, the CG approach seems to be sufficiently accurate to predict the location of the toxin, and can provide a starting configuration for more detailed atomistic simulations (or multiscale (75)) if the level of detail provided by the latter (76) is required. Furthermore, the somewhat sharp transition in the degree of deformation seen for a 1 Å movement of the toxin along the bilayer normal (Fig. 4) may in part reflect our simplified treatment of electrostatics. One can envisage that modified methods might yield a more gradual transition.

We must also consider how bilayer size might affect the magnitude of the deformations observed in this study. Our choice of bilayer size for VSTX-PC-free was selected as a trade-off between computational efficiency and the avoidance of periodicity artifacts. It would, however, be of interest to systematically investigate whether bilayer size could affect the magnitude of these deformations. Two further considerations involve the protein ionization state and the presence/absence of a TM voltage difference. Given that the protonation state of the charged residues of the toxin is dependent on their immediate environment, one could assign protonation states based on the position of the toxin along z and investigate the effects (if any) on the PMF profiles. It would also be of interest to investigate the sensitivity of the free energy profiles to changes in TM voltage (our simulations utilized a zero voltage).

We have shown for a relatively simple toxin/bilayer system that bilayer deformation can affect the interaction between an interfacially located protein and bilayer. This may be compared with the results of some recent simulation studies, also obtained via CG models, of protein-induced bilayer deformations and the effects of the bilayer on the orientation of embedded (i.e., TM) proteins (44,63,77,78). Thus, for both interfacial and TM proteins, bilayer deformations may play an important role in protein/membrane interactions. We have also shown that the free energy is dependent on the lipid species present in the bilayer. Extrapolating from the effects demonstrated here, such studies should therefore explicitly consider the bilayer environment and composition, the dynamic organization of the bilayer around a membrane protein, and their possible effects on biological function (50). Thus, membrane proteins should not be considered in isolation, separate from their bilayer environment. In particular, the malleable nature of a pure POPC bilayer and, by extension, other phospholipid bilayers provides an additional layer of complexity that must be considered in future investigations of membrane proteins, as emphasized by a number of recent simulations (7,44,71).

SUPPLEMENTARY MATERIAL

To view all of the supplemental files associated with this article, visit www.biophysj.org.

We thank Oliver Beckstein, Peter Bond, Ranjit Vijayan, and Christopher Yau for their advice and assistance, and Henry Chew for commenting on the manuscript. Research in M.S.P.S.'s laboratory is funded by the Biotechnology and Biological Sciences Research Council (the Membrane Protein Structure Initiative and the Oxford Centre for Integrative Systems Biology), the Engineering and Physical Sciences Research Council (the Integrative Biology Project and the Bionanotechnology IRC), and the Wellcome Trust. C.L.W. also acknowledges support from the Overseas Research Students Awards Scheme. We thank the UK National Grid Service for access to the computer facilities.

REFERENCES

1. White, S. H., and W. C. Wimley. 1999. Membrane protein folding and stability: physical principles. *Annu. Rev. Biophys. Biomol. Struct.* 28: 319–365.
2. Nina, M., S. Bernèche, and B. Roux. 2000. Anchoring of a monotopic membrane protein: the binding of prostaglandin H2 synthase-1 to the surface of a phospholipid bilayer. *Eur. Biophys. J.* 29:439–454.
3. Fowler, P. W., and P. V. Coveney. 2006. A computational protocol for the integration of the monotopic protein prostaglandin H2 synthase into a phospholipid bilayer. *Biophys. J.* 91:401–410.

4. Bhardwaj, N., R. V. Stahelin, G. Zhao, W. Cho, and H. Lui. 2007. MeTaDoR: a comprehensive resource for membrane targeting domains and their host proteins. *Bioinformatics*. 23:3110–3112.
5. Swartz, K. J. 2007. Tarantula toxins interacting with voltage sensors in potassium channels. *Toxicon*. 49:213–230.
6. Tatulian, S. A., S. Qin, A. H. Pande, and X. He. 2005. Positioning membrane proteins by novel protein engineering and biophysical approaches. *J. Mol. Biol.* 351:939–947.
7. Jaud, S., D. J. Tobias, J. J. Falke, and S. H. White. 2007. Self-induced docking site of a deeply embedded peripheral membrane protein. *Biophys. J.* 92:517–524.
8. Hille, B. 2001. Ionic Channels of Excitable Membranes. Sinauer Associates, Sunderland, MA. 814 p.
9. MacKinnon, R. 2003. Potassium channels. *FEBS Lett.* 555:62–65.
10. Jiang, Y., A. Lee, J. Chen, V. Ruta, M. Cadene, B. T. Chait, and R. Mackinnon. 2003. X-ray structure of a voltage-dependent K^+ channel. *Nature*. 423:33–41.
11. Jiang, Y., V. Ruta, J. Chen, A. G. Lee, and R. Mackinnon. 2003. The principle of gating charge movement in a voltage-dependent K^+ channel. *Nature*. 423:42–48.
12. Ruta, V., and R. MacKinnon. 2004. Localization of the voltage-sensor toxin receptor on KvAP. *Biochemistry*. 43:10071–10079.
13. Long, S. B., E. B. Campbell, and R. MacKinnon. 2005. Crystal structure of a mammalian voltage-dependent *Shaker* family K^+ channel. *Science*. 309:897–902.
14. Long, S. B., E. B. Campbell, and R. MacKinnon. 2005. Voltage sensor of Kv1.2: structural basis of electromechanical coupling. *Science*. 309:903–908.
15. Long, S. B., X. Tao, E. B. Campbell, and R. MacKinnon. 2007. Atomic structure of a voltage-dependent K^+ channel in a lipid membrane-like environment. *Nature*. 450:376–382.
16. Alabi, A. A., M. I. Bahamonde, H. J. Jung, H. J. Kim, and K. J. Swartz. 2007. Portability of paddle motif function and pharmacology in voltage sensors. *Nature*. 450:370–375.
17. Swartz, K. J., and R. Mackinnon. 1995. An inhibitor of the Kv2.1 potassium channel isolated from the venom of a Chilean tarantula. *Neuron*. 15:941–949.
18. Li-Smerin, Y., and K. J. Swartz. 1998. Gating modifier toxins reveal a conserved structural motif in voltage-gated Ca^{2+} and K^+ channels. *Proc. Natl. Acad. Sci. USA*. 95:8585–8589.
19. Cestele, S., Y. S. Qu, J. C. Rogers, H. Rochat, T. Scheuer, and W. A. Catterall. 1998. Voltage sensor-trapping: Enhanced activation of sodium channels by β-scorpion toxin bound to the S3–S4 loop in domain II. *Neuron*. 21:919–931.
20. Li-Smerin, Y., and K. J. Swartz. 2000. Localization and molecular determinants of the hanatoxin receptors on the voltage-sensing domains of a K^+ channel. *J. Gen. Physiol.* 115:673–684.
21. Takahashi, H., J. I. Kim, H. J. Min, K. Sato, K. J. Swartz, and I. Shimada. 2000. Solution structure of hanatoxin1, a gating modifier of voltage- dependent K^+ channels: common surface features of gating modifier toxins. *J. Mol. Biol.* 297:771–780.
22. Winterfield, J. R., and K. J. Swartz. 2000. A hot spot for the interaction of gating modifier toxins with voltage-dependent ion channels. *J. Gen. Physiol.* 116:637–644.
23. Lou, K. L., P. T. Huang, Y. S. Shiau, Y. C. Liaw, Y. Y. Shiau, and H. H. Liou. 2003. A possible molecular mechanism of hanatoxin binding-modified gating in voltage-gated K^+-channels. *J. Mol. Recognit.* 16:392–395.
24. Lee, S. Y., and R. MacKinnon. 2004. A membrane-access mechanism of ion channel inhibition by voltage sensor toxins from spider venom. *Nature*. 430:232–235.
25. Lee, H. C., J. M. Wang, and K. J. Swartz. 2004. Interaction between extracellular hanatoxin and the resting conformation of the voltage-sensor paddle in Kv channels. *Neuron*. 40:527–536.
26. Jung, H. J., J. Y. Lee, S. H. Kim, Y. J. Eu, S. Y. Shin, M. Milescu, K. J. Swartz, and J. I. Kim. 2005. Solution structure and lipid membrane partitioning of VSTx1, an inhibitor of the KvAP potassium channel. *Biochemistry*. 44:6015–6023.
27. Catterall, W. A., S. Cestèle, V. Yarov-Yarovoy, F. H. Yu, K. Konoki, and T. Scheuer. 2007. Voltage-gated ion channels and gating modifier toxins. *Toxicon*. 49:124–141.
28. Milescu, M., J. Vobecky, S. H. Roh, S. H. Kim, H. J. Jung, J. Il Kim, and K. J. Swartz. 2007. Tarantula toxins interact with voltage sensors within lipid membranes. *J. Gen. Physiol.* 130:497–511.
29. Ruta, V., Y. X. Jiang, A. Lee, J. Y. Chen, and R. MacKinnon. 2003. Functional analysis of an archaebacterial voltage-dependent K^+ channel. *Nature*. 422:180–185.
30. Bemporad, D., C. L. Wee, Z. Sands, A. Grottesi, and M. S. P. Sansom. 2006. VSTx1, a modifier of Kv channel gating, localizes to the interfacial region of lipid bilayers. *Biochemistry*. 45:11844–11855.
31. Wee, C. L., D. Bemporad, Z. A. Sands, D. Gavaghan, and M. S. P. Sansom. 2007. SGTx1, a Kv channel gating-modifier toxin, binds to the interfacial region of lipid bilayers. *Biophys. J.* 92:L07–L09.
32. Shelley, J. C., M. Y. Shelley, R. C. Reeder, S. Bandyopadhyay, and M. L. Klein. 2001. A coarse grain model for phospholipid simulations. *J. Phys. Chem. B*. 105:4464–4470.
33. Whitehead, L., C. M. Edge, and J. W. Essex. 2001. Molecular dynamics simulation of the hydrocarbon region of a biomembrane using a reduced representation model. *J. Comput. Chem.* 22:1622–1633.
34. Stevens, M. J., J. H. Hoh, and T. B. Woolf. 2003. Insights into the molecular mechanism of membrane fusion from simulation: evidence for the association of splayed tails. *Phys. Rev. Lett.* 91:188102.
35. Marrink, S. J., A. H. de Vries, and A. E. Mark. 2004. Coarse grained model for semiquantitative lipid simulations. *J. Phys. Chem. B*. 108: 750–760.
36. Murtola, T., E. Falck, M. Patra, M. Karttunen, and I. Vattulainen. 2004. Coarse-grained model for phospholipid/cholesterol bilayer. *J. Chem. Phys.* 121:9156–9165.
37. Stevens, M. J. 2004. Coarse-grained simulations of lipid bilayers. *J. Chem. Phys.* 121:11942–11948.
38. Nielsen, S. O., C. F. Lopez, G. Srinivas, and M. L. Klein. 2004. Coarse grain models and the computer simulation of soft materials. *J. Phys. Condens. Matter*. 16:R481–R512.
39. Shi, Q., S. Izvekov, and G. A. Voth. 2006. Mixed atomistic and coarse-grained molecular dynamics: simulation of a membrane bound ion channel. *J. Phys. Chem. B*. 110:15045–15048.
40. Shih, A. Y., A. Arkhipov, P. L. Freddolino, and K. Schulten. 2006. Coarse grained protein-lipid model with application to lipoprotein particles. *J. Phys. Chem. B*. 110:3674–3684.
41. Marrink, S. J., J. Risselada, S. Yefimov, D. P. Tieleman, and A. H. de Vries. 2007. The MARTINI forcefield: coarse grained model for biomolecular simulations. *J. Phys. Chem. B*. 111:7812–7824.
42. Bond, P. J., and M. S. P. Sansom. 2007. Bilayer deformation by the Kv channel voltage sensor domain revealed by self-assembly simulations. *Proc. Natl. Acad. Sci. USA*. 104:2631–2636.
43. Reynwar, B. J., G. Illya, V. A. Harmandaris, M. M. Müller, K. Kremer, and M. Deserno. 2007. Aggregation and vesiculation of membrane proteins by curvature-mediated interactions. *Nature*. 447: 461–464.
44. Periole, X., T. Huber, S. J. Marrink, and T. P. Sakmar. 2007. G protein-coupled receptors self-assemble in dynamics simulations of model bilayers. *J. Am. Chem. Soc.* 129:10126–10132.
45. Han, W., and Y. D. Wu. 2007. Coarse-grained protein model coupled with a coarse-grained water model: molecular dynamics study of polyalanine-based peptides. *J. Chem. Theory Comput.* 3:2146–2161.
46. Bond, P. J., and M. S. P. Sansom. 2006. Insertion and assembly of membrane proteins via simulation. *J. Am. Chem. Soc.* 128:2697–2704.
47. Bond, P. J., J. Holyoake, A. Ivetac, S. Khalid, and M. S. P. Sansom. 2007. Coarse-grained molecular dynamics simulations of membrane proteins and peptides. *J. Struct. Biol.* 157:593–605.

48. Yefimov, S., E. van der Giessen, P. R. Onck, and S. J. Marrink. 2008. Mechanosensitive membrane channels in action. *Biophys. J.* 94:2994–3002.

49. Sperotto, M. M., S. May, and A. Baumgaertner. 2006. Modelling of proteins in membranes. *Chem. Phys. Lipids.* 141:2–29.

50. Andersen, O. S., and R. E. Koeppe. 2007. Bilayer thickness and membrane protein function: an energetic perspective. *Annu. Rev. Biophys. Biomol. Struct.* 36:107–130.

51. Roux, B. 1995. The calculation of the potential of mean force using computer simulations. *Comput. Phys. Commun.* 91:275–282.

52. Kumar, S., D. Bouzida, R. H. Swendsen, P. A. Kollman, and J. M. Rosenberg. 1992. The weighted histogram analysis method for free-energy calculations on biomolecules. 1. The method. *J. Comput. Chem.* 13:1011–1021.

53. Bond, P. J., C. L. Wee, and M. S. P. Sansom. 2008. Coarse-grained molecular dynamics simulations as an approach to the energetics of helix insertion into a bilayer. *Biochemistry.* In press.

54. Marrink, S. J., J. Risselada, and A. E. Mark. 2005. Simulation of gel phase formation and melting in lipid bilayers using a coarse grained model. *Chem. Phys. Lipids.* 135:223–244.

55. Lindahl, E., B. Hess, and D. van der Spoel. 2001. GROMACS 3.0: a package for molecular simulation and trajectory analysis. *J. Mol. Model.* 7:306–317.

56. van der Spoel, D., E. Lindahl, B. Hess, G. Groenhof, A. E. Mark, and H. J. Berendsen. 2005. GROMACS: fast, flexible, and free. *J. Comput. Chem.* 26:1701–1718.

57. Berendsen, H. J. C., J. P. M. Postma, W. F. van Gunsteren, A. DiNola, and J. R. Haak. 1984. Molecular dynamics with coupling to an external bath. *J. Chem. Phys.* 81:3684–3690.

58. Eisenberg, D., E. Schwarz, M. Komaromy, and R. Wall. 1984. Analysis of membrane and surface protein sequences with the hydrophobic moment plot. *J. Mol. Biol.* 179:125–142.

59. Phillips, L. R., M. Milescu, Y. Li-Smerin, J. A. Midell, J. I. Kim, and K. J. Swartz. 2005. Voltage-sensor activation with a tarantula-toxin as cargo. *Nature.* 436:857–860.

60. Dan, F., and S. A. Safran. 1998. Effect of lipid characteristics on the structure of transmembrane proteins. *Biophys. J.* 75:1410–1414.

61. Hyvönen, M. J., and P. T. Kovanen. 2005. Molecular dynamics simulations of unsaturated lipid bilayers: effects of varying the numbers of double bonds. *Eur. Biophys. J.* 34:294–305.

62. Dorairaj, S., and T. W. Allen. 2007. On the thermodynamic stability of a charged arginine side chain in a transmembrane helix. *Proc. Natl. Acad. Sci. USA.* 104:4943–4948.

63. Scott, K. A., P. J. Bond, A. Ivetac, A. P. Chetwynd, S. Khalid, and M. S. P. Sansom. 2008. Coarse-grained MD simulations of membrane protein-bilayer self-assembly. *Structure.* 16:621–630.

64. Bernèche, S., and B. Roux. 2001. Energetics of ion conduction through the K^+ channel. *Nature.* 414:73–77.

65. Beckstein, O., and M. S. P. Sansom. 2006. A hydrophobic gate in an ion channel: the closed state of the nicotinic acetylcholine receptor. *Phys. Biol.* 3:147–159.

66. MacCallum, J. L., W. F. D. Bennett, and D. P. Tieleman. 2007. Partitioning of amino acid side chains into lipid bilayers: results from computer simulations and comparison to experiment. *J. Gen. Physiol.* 129:371–377.

67. Ben-Tal, N., B. Honig, R. M. Peitzsch, G. Denisov, and S. McLaughlin. 1996. Binding of small basic peptides to membrane containing acidic lipids: theoretical models and experimental results. *Biophys. J.* 71: 561–575.

68. Posokhov, Y. O., P. A. Gottlieb, M. J. Morales, F. Sachs, and A. S. Ladokhin. 2007. Is lipid bilayer binding a common property of inhibitor cysteine knot ion-channel blockers? *Biophys. J.* 93:L20–L22.

69. Monticelli, L., S. K. Kandasamy, X. Periole, R. G. Larson, D. P. Tieleman, and S. J. Marrink. 2008. The MARTINI coarse grained force field: extension to proteins. *J. Comput. Theor. Chem.* 4:819–834.

70. MacCallum, J. L., W. F. D. Bennett, and D. P. Tieleman. 2008. Distribution of amino acids in a lipid bilayer from computer simulations. *Biophys. J.* 94:3393–3404.

71. Freites, J. A., D. J. Tobias, G. von Heijne, and S. H. White. 2005. Interface connections of a transmembrane voltage sensor. *Proc. Natl. Acad. Sci. USA.* 102:15059–15064.

72. Sands, Z. A., and M. S. P. Sansom. 2007. How does a voltage-sensor interact with a lipid bilayer? Simulations of a potassium channel domain. *Structure.* 15:235–244.

73. Krepkiy, D., E. Mihailescu, K. Gawrisch, and K. J. Swartz. 2007. Influence of a potassium channel voltage sensor toxin on the structure of lipid membranes. *Biophys. J.* :295a. (Abstr.)

74. Allen, T. W. 2007. Modeling charged protein side chains in lipid membranes. *J. Gen. Physiol.* 130:237–240.

75. Ayton, G. S., and G. A. Voth. 2007. Multiscale simulation of transmembrane proteins. *J. Struct. Biol.* 157:570–578.

76. Nishizawa, M., and K. Nishizawa. 2007. Molecular dynamics simulations of a stretch-activated channel inhibitor GsMTx4 with lipid membranes: two binding modes and effects of lipid structure. *Biophys. J.* 92: 4233–4243.

77. Nielsen, S. O., B. Ensing, V. Ortiz, P. B. Moore, and M. L. Klein. 2005. Lipid bilayer perturbations around a transmembrane nanotube: a coarse grain molecular dynamics study. *Biophys. J.* 88:3822–3828.

78. Venturoli, M., B. Smit, and M. M. Sperotto. 2005. Simulation studies of protein-induced bilayer deformations, and lipid-induced protein tilting, on a mesoscopic model for lipid bilayers with embedded proteins. *Biophys. J.* 88:1778–1798.